Angular dependence of neutrino emission from rotating black holes

D. A. Leahy and W. G. Unruh
The University of British Columbia, Vancouver V6T 1W5, British Columbia, Canada
(Received 16 January 1979)

The asymmetry of the angular dependence of neutrino emission from rotating black holes is calculated. A low-frequency analytic approximation demonstrates the preferential emission of neutrinos (antineutrinos) antiparallel (parallel) to the direction of the black hole's angular momentum vector. Numerical calculations are performed to reveal the detailed nature of the neutrino emission on polar angle, neutrino energy, and black-hole angular momentum and mass.

I. INTRODUCTION

Quantum theory predicts that black holes emit a thermal spectrum of particles into the surrounding vacuum.[1] Kerr (rotating) black holes lose angular momentum in addition to mass due to the particle emission process. As a result, particles with positive helicity[3] are emitted preferentially along the rotation axis in the direction of the angular momentum vector of the black hole and negative-helicity particles in the opposite direction.

Most particles occur in nature with both signs of helicity due to invariance under the parity operator. However, neutrinos violate parity maximally, occurring only with negative helicity.[4] *CP* invariance then gives the antineutrino a positive helicity. The result is that neutrinos are preferentially emitted from the "southern" hemisphere and antineutrinos from the "northern" hemisphere during the evaporation of a rotating black hole. The importance of parity violation by neutrinos in the presence of a Kerr black hole was pointed out by Unruh[5] and has been independently investigated by Vilenkin.[6]

In this paper, a low-frequency analytic approximation is made to verify the asymmetry in neutrino emission. The results of numerical calculations involving the full set of equation are presented.[7] These display the detailed dependence of the emission on polar angle (θ), neutrino energy (ω), and black-hole angular momentum (J) and mass (M).

Natural (Planck) units in which $h=c=G=k=1$ are used throughout, except as noted. For the conversion to more common units see the last (red) page of Misner *et al.*[8]

II. THEORETICAL FORMULATION

The minimally coupled neutrino field equations[9] describe the propagation of the classical neutrino field in a fixed background metric, which in our case is that of a Kerr black hole. Boyer-Lindquist coordinates[10] are used, in which the neutrino equations were first shown to be separable.[5] The formal calculations follow those of Unruh.[11] However, the orbital quantum number m is opposite in sign to that of Ref. 11. In particular, the neutrino field normal modes take the form (with $x^0=t$, $x^1=\theta$, $x^2=\phi$, $x^3=r$)

$$\psi(x^\mu;\ \omega,m,k,\lambda)=\frac{e^{-i\omega t}e^{+im\phi}}{[\Delta\sin^2\theta(r+ia\cos\theta)^2]^{1/4}}\begin{bmatrix}\eta\\ \eta\end{bmatrix},\qquad \eta=\begin{bmatrix}R_1(r) & S_1(\theta)\\ R_2(r) & S_2(\theta)\end{bmatrix}. \tag{2.1}$$

The radial and angular functions, R and S, satisfy Eqs. (2.20) and (2.21) of Ref. 11:

$$\left(\frac{d}{dr}-\frac{i}{\Delta}[\omega(r^2+a^2)-ma]\right)R_1(r)=\frac{k}{\Delta^{1/2}}R_2(r),\qquad \left(\frac{d}{dr}+\frac{i}{\Delta}[\omega(r^2+a^2)-ma]\right)R_2(r)=\frac{k}{\Delta^{1/2}}R_1(r); \tag{2.2}$$

$$\left[\frac{d}{d\theta}+\left(a\omega\sin\theta-\frac{m}{\sin\theta}\right)\right]S_1(\theta)=kS_2(\theta),\qquad \left[\frac{d}{d\theta}-\left(a\omega\sin\theta-\frac{m}{\sin\theta}\right)\right]S_2(\theta)=-kS_1(\theta), \tag{2.3}$$

where $a=J/M$, the angular momentum per unit mass of the black hole, and $\Delta=r^2-2Mr+a^2$.

Linearly independent solutions to (2.2), denoted by $(R_1^\lambda(r),\ R_2^\lambda(r))$ with $\lambda=\pm$, have asymptotic forms [Ref. 11, Eq. (2.23)]:

$$(R_1^+(r),R_2^+(r))\sim\frac{1}{\sqrt{2\pi}}\times\begin{cases}(A_+(\omega,m,k)e^{i\omega\hat r},\ e^{-i\omega\hat r}), & \hat r\to\infty\\ (0,\ B_+(\omega,m,k)e^{-i\hat\omega\hat r}), & \hat r\to-\infty,\end{cases} \tag{2.4}$$

$$(R_1^-(r),R_2^-(r))\sim\frac{1}{\sqrt{2\pi}}\times\begin{cases}(B_-(\omega,m,k)e^{i\omega\hat r},\ 0) & \hat r\to\infty\\ (e^{i\hat\omega\hat r},\ A_-(\omega,m,k)e^{-i\hat\omega\hat r}), & \hat r\to-\infty.\end{cases}$$

In (2.4) $\hat r$ is defined by $d\hat r/dr=(r^2+a^2)/\Delta$ and approaches $-\infty$ as r approaches the outer event horizon. One also has

$$\hat{\omega} = \omega - m\omega_H, \quad \omega_H = a(2M^2\{1+[1-(a/M)^2]^{1/2}\})^{-1}. \tag{2.5}$$

ω_H is the angular velocity of the outer horizon. The $\lambda = +$ solutions in (2.4) represent waves incoming from infinity which are reflected with amplitude A_+ and transmitted to the horizon with amplitude B_+. The $\lambda = -$ solutions represent waves outgoing from the horizon.

S_1 and S_2 in (2.3) possess the symmetries

$$(S_1(m,k,a\omega,\pi-\theta), S_2(m,k,a\omega,\pi-\theta) = \pm(S_2(m,k,a\omega,\theta), S_1(m,k,a\omega,\theta)), \tag{2.6a}$$

$$(S_1(-m,k,-a\omega,\theta), S_2(-m,k,-a\omega,\theta)) = \pm(S_2(m,k,a\omega,\theta), -S_1(m,k,a\omega,\theta)), \tag{2.6b}$$

$$(S_1(m,-k,a\omega,\theta), S_2(m,-k,a\omega,\theta)) = \pm(S_1(m,k,a\omega,\theta), -S_2(m,k,a\omega,\theta)). \tag{2.6c}$$

Because of (2.6c) one can always take k positive, which we do. S_1 and S_2 are related to the spin-weighted spheroidal harmonics of Press and Teukolsky[16] by

$$S_1(m,k,a\omega,\theta) = \left(\frac{\sin\theta}{2}\right)^{1/2} {}_{-1/2}S_l^m(\theta,a\omega),$$
$$S_2(m,k,a\omega,\theta) = \left(\frac{\sin\theta}{2}\right)^{1/2} {}_{1/2}S_l^m(\theta,a\omega). \tag{2.7}$$

In (2.7) l is the value of k for $a\omega = 0$ and is used to denumerate the k eigenvalues. l takes on half-integral values $(\frac{1}{2}, \frac{3}{2}, \frac{5}{2}, \ldots)$ and for given l, m takes on the $2l+1$ values $(-l, -l+1, \ldots, +l)$. l is the total angular momentum quantum number (spin plus orbital) for a nonrotating black hole while m is the component of angular momentum along the rotation axis.

The quantization procedure involves making the neutrino field an operator and expanding it in terms of positive-frequency modes and creation and annihilation operators. The choice of positive frequency is not unambiguous in a nonflat spacetime, yet it determines the vacuum state of the field.[12] Hawking[1] demonstrated the correct choice for black holes formed by stellar collapse. Unruh[13] developed an equivalent definition of positive frequency for the full analytic extension[14] of the Kerr metric. The latter definition is mathematically simpler and is used here: Ingoing modes, as given by Eq. (2.1) with $\lambda = +$, are positive frequency for $\omega > 0$ (the standard flat-space definition); positive-frequency outgoing modes ($\lambda = -1$) are of the form

$$\frac{\exp(\pi\hat{\omega}/2K_+)}{[2\cosh(\pi\hat{\omega}/K_+)]^{1/2}}\psi(x^\mu,\omega,m,k,-) \tag{2.8}$$

in the region outside the horizon, where ω takes on all values, positive and negative. In (2.8) K_+ is the surface gravity of the outer horizon of the black hole:

$$K_+ = 2M\{1+[1-(a/M)^2]^{-1/2}\}. \tag{2.9}$$

Negative-frequency modes for $\lambda = -$ are of the form (2.8) but with $\hat{\omega}$ replaced by $-\hat{\omega}$.

The field operator Ψ then has the following expansion outside the horizon in terms of the above normal modes:

$$\Psi(x^\mu) = \sum_{l,m}\left\{\int_{\omega>0} d\omega[\psi(x^\mu;\omega,m,k,+)a(\omega,m,k,+) + \psi(x^\mu;-\omega,-m,k,+)b^\dagger(\omega,m,k,+)] + \int_{\text{all}\,\omega}\frac{d\omega}{[2\cosh(\pi\hat{\omega}/K_+)]^{1/2}}\left[\exp\left(\frac{\pi\hat{\omega}}{2K_+}\right)a(\omega,m,k,-) + \exp\left(\frac{-\pi\hat{\omega}}{2K_+}\right)b^\dagger(\omega,m,k,-)\right]\psi(x^\mu;\omega,m,k,-)\right\}. \tag{2.10}$$

Some physical quantities of interest are the expectation values of the current and energy-momentum operators J^μ and $T_{\mu\nu}$. These are functions[15] of the field operator Ψ:

$$J^\mu(x^\mu) = \tfrac{1}{2}[\bar{\Psi}, \gamma^\mu\Psi],$$
$$T_{\mu\nu}(x^\mu) = \tfrac{1}{4}i[\bar{\Psi}, \gamma_{(\mu}\nabla_{\nu)}\Psi] + \text{Hermitian conjugate}. \tag{2.11}$$

J^μ is a conserved current. The symmetry of the Kerr metric under translations in t and ϕ coordinates give rise to two other conserved currents T_t^μ and T_ϕ^μ. The radial components of these three currents are the flows of the number of neutrinos minus the number of antineutrinos, $N_{\nu-\bar{\nu}}$; energy, E; and angular momentum, L, respectively, in the radial direction away from the black hole. In the vacuum state one has

$$\frac{d^2N_{\nu-\bar{\nu}}(x^\mu)}{r^2d\Omega dt} = \langle 0|J^r(x^\mu)|0\rangle, \tag{2.12a}$$

$$\frac{d^2E(x^\mu)}{r^2d\Omega dt} = \langle 0|T_t^r(x^\mu)|0\rangle, \tag{2.12b}$$

$$\frac{d^2L(x^\mu)}{r^2d\Omega dt} = \langle 0|T_\phi^r(x^\mu)|0\rangle. \tag{2.12c}$$

Substitution of (2.10) and (2.11) into (2.12) yields explicit formulas for the quantities in (2.12). The large-r asymptotic forms of the radial functions

(2.4) are then put into the resulting formulas to give values for the quantities in (2.12) far from the rotating black hole. These can then be expressed in dimensionless form by factoring out the mass M of the black hole:

$$M\frac{d^2N_{\nu-\bar{\nu}}}{d\Omega dt}(\alpha,\theta)=\frac{1}{2\pi}\sum_{lm}\int_{x>0}dx f(x)g(\theta)(S_1^2-S_2^2), \tag{2.13a}$$

$$M\frac{d^2N_{\nu+\bar{\nu}}}{d\Omega dt}(\alpha,\theta)=\frac{1}{2\pi}\sum_{lm}\int_{x>0}dx f(x)g(\theta)(S_1^2+S_2^2), \tag{2.13b}$$

$$-M^2\frac{d^2E(\alpha,\theta)}{d\Omega dt}=\frac{1}{2\pi}\sum_{l,m}\int_{x>0}dx\,xf(x)g(\theta)(S_1^2+S_2^2), \tag{2.13c}$$

$$-M\frac{d^2L(\alpha,\theta)}{d\Omega dt}=\frac{1}{2\pi}\sum_{l,m}\int_{x>0}dx f(x)g(\theta)\times\left[\frac{m-\alpha x\sin^2\theta}{2}(S_1^2+S_2^2)+k\sin\theta S_1S_2+\frac{\cos\theta}{4}(S_1^2-S_2^2)\right], \tag{2.13d}$$

with $\alpha=a/M$, $x=M\omega$, $g(\theta)=2/\sin\theta$, and

$$f(x)=|B_-(\alpha,x,m,k)|^2[\exp(2\pi\hat{\omega}/K_+)+1]^{-1}.$$

$|B_-|^2$ is the transmission probability for a neutrino wave originating at the past horizon to reach infinity or for a wave originating at infinity to be absorbed by the black hole and is found by solving the radial equations (2.2) for $R_1(r)$ and $R_2(r)$. $N_{\nu+\bar{\nu}}$ is the number of neutrinos plus antineutrinos. $S_1(m,k,\alpha x,\theta)$ and $S_2(m,k,\alpha x,\theta)$ are the angular eigenfunctions involved in the separation of ψ into normal modes in (2.1). Integrated over angle, equations (2.13) yield the loss rates[2] through a spherical 2-surface at large r:

$$-M\frac{dN_{\nu-\bar{\nu}}}{dt}(\alpha)=0, \tag{2.14a}$$

$$-M\frac{dN_{\nu+\bar{\nu}}}{dt}(\alpha)=\frac{1}{2\pi}\sum_{l,m}\int_{x>0}dx f(x), \tag{2.14b}$$

$$-M^2\frac{dE}{dt}(\alpha)=\frac{1}{2\pi}\sum_{l,m}\int_{x>0}dx\,xf(x), \tag{2.14c}$$

$$-M\frac{dL(\alpha)}{dt}=\frac{1}{2\pi}\sum_{l,m}\int_{x>0}dx\,mf(x). \tag{2.14d}$$

The Fermi-Dirac factor $[\exp(2\pi\hat{\omega}/K_+)+1]^{-1}$ in (2.13) and (2.14) [through $f(x)$] is responsible for the famous thermal character, with temperature $K_+/2\pi$, of the black-hole emission.[1] Departures from a pure thermal distribution are due to the albedo of the black hole varying with frequency through $|B_-|^2$ and to the quantum instability associated with the rotation of the black hole[11] (i.e., the presence of $\hat{\omega}$ rather than ω in the Fermi-Dirac factor).

III. LOW-FREQUENCY ANALYTIC APPROXIMATION

The solutions of the wave equation, and hence the angular eigenfunctions and the transmission coefficients, cannot be expressed in terms of known analytic functions. However, for $x=M\omega=0$ both radial and angular functions can be found exactly and the lowest-order corrections to these functions for nonzero x can be obtained. Page[2] gives the transmission probabilities $|B_-|^2$ (his Γ) for $x\ll 1$. Because the transmission probabilites for the various l modes go as x^{2l+1}, only the lowest values of l will contribute to the emission rate for small values of x. In particular we have

$$\begin{aligned}|B_-(m,\tfrac{1}{2},\alpha,x)|^2&\simeq x^2,\\ |B_-(m,\tfrac{3}{2},\alpha,x)|^2&\simeq(1+\tfrac{1}{9}\alpha^2)(1-\alpha^2)^{\frac{1}{4}}x^4.\end{aligned} \tag{3.1}$$

We must also find S_1 and S_2 to lowest order in $\alpha x=a\omega$. S_1 and S_2 are directly related [Eq. (2.7)] to the spin-weighted spheroidal harmonics which for $x=0$ reduce to the spin-weighted spherical harmonics ${}_s\gamma_l^m(\theta)$. Following Press and Teukolsky[16] we expand the spheroidal harmonics in terms of the spherical harmonics:

$${}_{1/2}S_l^m(\theta,\alpha x)={}_{1/2}Y_l^m(\theta)+\sum_{l'\neq l}{}_{1/2}A_{ll'}^m(\alpha x)\,{}_{1/2}Y_{l'}^m(\theta). \tag{3.2}$$

Since the $l=\frac{1}{2}$ term dominates the transmission probability because of the radial dependence on x, we need only consider this mode. For $m=+\frac{1}{2}$, we have

$${}_{1/2}A_{ll'}^{1/2}\approx\alpha x\left(\frac{[(l+\frac{1}{2})(l+\frac{3}{2})]^{1/2}}{(2l+2)^2}\delta_{l',l+1}+\frac{[(l-\frac{1}{2})(l+\frac{1}{2})]^{1/2}}{(2l)^2}\delta_{l',l-1}\right). \tag{3.3}$$

Using the equations[17] for the ${}_sY_l^m$,

$${}_{1/2}Y_{1/2}^{1/2}(\theta)=\frac{1}{\sqrt{2\pi}}\sin\frac{\theta}{2},$$

$${}_{1/2}Y_{3/2}^{1/2}(\theta)=\frac{1}{\sqrt{\pi}}\sin\frac{\theta}{2}\cos\theta,$$

Eqs. (3.2), (3.3), and the symmetries (2.6), we find

$$\begin{aligned}{}_{1/2}S_{1/2}^{1/2}(\theta,\alpha x)&\simeq\frac{1}{\sqrt{2\pi}}\sin\frac{\theta}{2}(1+\alpha x\tfrac{2}{9}\cos\theta),\\ {}_{-1/2}S_{1/2}^{1/2}(\theta,\alpha x)&\simeq\frac{1}{\sqrt{2\pi}}\cos\frac{\theta}{2}(1-\alpha x\tfrac{2}{9}\cos\theta),\\ {}_{1/2}S_{1/2}^{-1/2}(\theta,\alpha x)&\simeq\frac{-1}{\sqrt{2\pi}}\cos\frac{\theta}{2}(1+\alpha x\tfrac{2}{9}\cos\theta),\\ {}_{-1/2}S_{1/2}^{-1/2}(\theta,\alpha x)&\simeq\frac{-1}{\sqrt{2\pi}}\sin\frac{\theta}{2}(1-\alpha x\tfrac{2}{9}\cos\theta).\end{aligned} \tag{3.4}$$

Substitution of Eqs. (3.4) and (3.1) into (2.13a) yields the neutrino number emission rate per unit frequency to order x^3:

$$\frac{d^2N_{\nu-\bar{\nu}}}{d\Omega dt d\omega} \simeq \frac{x^2}{(2\pi)^2}\left\{\left[\exp\left(\frac{2\pi(\omega+\omega_H/2)}{K_+}\right)+1\right]^{-1}(1+\tfrac{4}{9}\alpha x) - \left[\exp\left(\frac{2\pi(\omega-\omega_H/2)}{K_+}\right)+1\right]^{-1} \times (1-\tfrac{4}{9}\alpha x)\right\}\cos\theta . \quad (3.5)$$

The dominant contribution to the asymmetry exhibited by (3.5) is the exponential factor which arises from the quantum instability of rotating black holes.[11]

For a slowly rotating black hole, $\alpha \ll 1$, (3.5) reduces to

$$\frac{d^2N_{\nu-\bar{\nu}}(\alpha,\theta)}{d\Omega dt d\omega} \simeq -\left(\frac{x}{2\pi}\right)^2 \frac{\pi\alpha}{2(1-\alpha^2)^{1/2}}\cos\theta . \quad (3.6)$$

For a rapidly rotating black hole, $(1-\alpha^2)^{1/2} \ll 1$, one has

$$\frac{d^2N_{\nu-\bar{\nu}}(\alpha,\theta)}{d\Omega dt d\omega} \simeq -\left(\frac{x}{2\pi}\right)^2 \cos\theta . \quad (3.7)$$

The dependence on α is linear for small α and constant for $\alpha \to 1$. For arbitrary rotation, Eq. (3.5) gives the emission rate as a simple analytic function of α. The angular dependence in the low-frequency limit is given by the $\cos\theta$ factor, verifying the asymmetry in emission. The asymmetry is not sharply peaked in angle θ. Neutrinos dominate in the hemisphere $\theta < \pi/2$, antineutrinos in the hemisphere $\theta > \pi/2$, as expected.

IV. NUMERICAL CALCULATIONS

The emission rates have also been evaluated for arbitrary values of $x = M\omega$ by solving for the angular eigenfunctions S_1 and S_2 and for the transmission coefficients numerically. The results of a representative sample of the calculations will be presented here. More details about the calculations and further results will be presented in the thesis of one of us (D.L.).

The angular functions were calculated by direct numerical integration of the angular equations (2.3) using values for the eigenvalues k obtained from Page's[18] polynomial fits to his numerical calculations. Twenty-one (l, m) modes were calculated for about 10 values of αx from 0 to 3.

In each case, $S_1(\theta)$ and $S_2(\theta)$ were calculated for 41 distinct values of θ from 0.001 to $\pi/2$. The symmetry of these functions (2.6) under $\theta \to \pi - \theta$ and cubic spline interpolation were used for other values of θ and for other values of αx.

The transmission probabilities $|B_-(m, k, \alpha, x)|^2$ were calculated using the method described by Page.[19] These functions were calculated for the 21 (l, m) modes and for each of 15 values of α from 0.01 to 0.999. The double precision numerical integration routine UBC DDE[20] was used to solve the radial equations, with fractional and absolute error criteria of 10^{-6}. The frequencies x at which $|B_-|^2$ was calculated for each set of α, l, m values were chosen so as to make the estimated fractional error in the quantity $\int_{x>0} dx f(x)$ less than 10^{-4}. A list of values of M^2dE/dt and $MdN_{\nu+\bar{\nu}}/dt$ for a large number of α, l, m values, provided by Page, served as a check on the results.

V. RESULTS AND DISCUSSION

Representative results of the calculations are summarized with the help of the accompanying figures. Figure 1 shows the frequency dependence of the thermal Fermi-Dirac factor and of the transmission probability $|B_-|^2$ for the case $\alpha = a/M = 0.8$, $(l, m) = (\frac{3}{2}, \frac{3}{2})$. The effective temperature of the Fermi-Dirac factor $K_+/2\pi$ determines the slope of the cutoff in this factor. The case plotted has an effective temperature of $0.38/4\pi M$. For larger values of α the slope becomes steeper, and the factor approaches a step function as α approaches 1. The location of the drop is around $\omega = m\omega_H$ where this factor equals $\frac{1}{2}$.

The transmission probability is small for low frequency—for $\omega \gtrsim l\omega_H$ the neutrino wave does not have enough energy to surmount the gravitational-angular momentum barrier associated with the radial equations—and thereafter rises rapidly to unity.

The product of the Fermi-Dirac function and the transmission probability gives $f(x)$, which is proportional to the emission rate of particles for that given mode [Eq. (2.14b)]. This is displayed in Fig. 1(b). Because of the small overlap between the two functions, this probability is always much less than 1 for any mode, and is significant only over a very narrow frequency range.

The Fermi-Dirac function depends strongly on m (the cutoff occurs at $\omega = m\omega_H$) while the transmission coefficients depend only weakly on m. For $m < l$, the Fermi cutoff occurs long before the transmission probability becomes nonzero. Only if $\alpha = a/M$ is extremely small, giving a smaller slope to the Fermi-Dirac cutoff, will the $m \neq l$ modes contribute significantly. For larger α, it is only the $m = l$ mode which contributes to the emission.

The power spectrum summed over modes and integrated over angle,

$$M\frac{d^2E}{dtd\omega} = \frac{1}{2\pi}\sum_{l,m} x f(x) ,$$

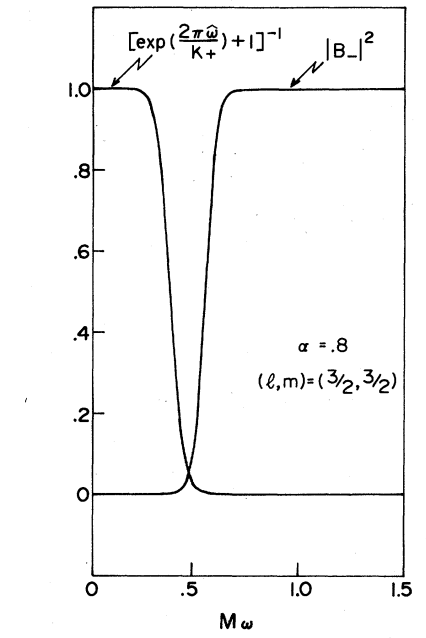

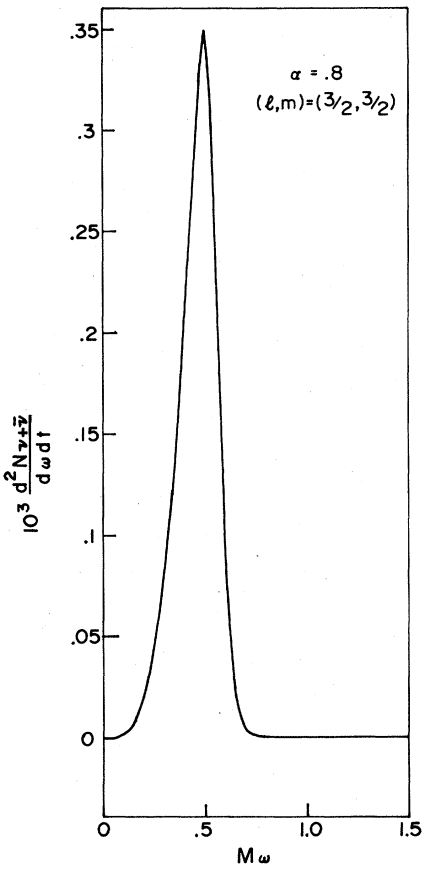

FIG. 1. (a) Fermi-Dirac factor and transmission probability $|B_-|^2$ for rotation parameter $\alpha = 0.8$ and angular mode $(l,m)=(\frac{3}{2},\frac{3}{2})$ vs frequency $M\omega$. (b) Single mode $(l,m)=(\frac{3}{2},\frac{3}{2})$ total number rate spectrum for $\alpha = 0.8$.

is given in Fig. 2 for $\alpha = 0$, 0.8, and 0.999. Only the lowest-order $l=\frac{1}{2}$ modes contribute to the mode sums in (2.13) and (2.14) for small α. Higher l modes increase in importance for increasing rotation. For $\alpha \gtrsim 0.9$, the power in the higher modes becomes greater than that in the $l=m=\frac{1}{2}$ mode. The peaks at increasing frequency for $\alpha = 0.999$ in Fig. 2 correspond to $l=m$ modes for $l=\frac{1}{2}$, $\frac{3}{2}$, $\frac{5}{2}$, $\frac{7}{2}$, $\frac{9}{2}$, and $\frac{11}{2}$, respectively. They appear as distinct spikes due to the sharp cutoff at $m\omega_H$ of the Fermi-Dirac factor and to the sharp rise of $|B_-|^2$ for $x \lesssim l\omega_H$ as noted in Figs. 1(a) and 1(b). The oscillations within the spikes are due to the frequency variation of $|B_-|^2$.

This shape of the power spectrum is not uniform in the angle θ. At the poles only the $l=m=\frac{1}{2}$ angular mode is nonzero and only that one peak would be seen in the power spectrum. Each of the higher l modes has its dominant angular peak nearer to the equator. Thus the number of peaks seen in the power spectrum will increase as one approaches $\theta = \pi/2$, and the spectrum will be dominated by the higher values of l near the equator.

The angular dependence of the net number current, i.e., neutrinos minus antineutrinos, is presented in Fig. 3(a) for $\alpha = 0.1$, 0.5, 0.8, and 0.999 while Fig. 3(b) displays the asymmetry in neutrino emission. This is defined as the ratio of the rates for $N_{\nu-\bar{\nu}}$ and $N_{\nu+\bar{\nu}}$ given in Eqs. (2.13a) and (2.13b). For even small values of α it is significant. In all cases the asymmetry is smooth in θ,

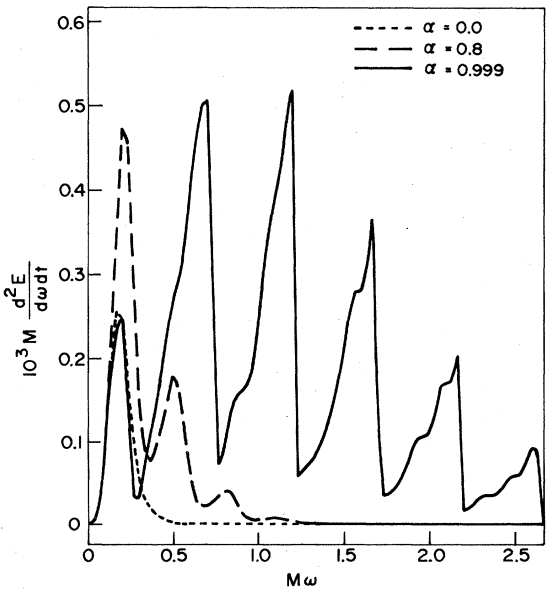

FIG. 2. Power spectrum for $\alpha = 0$, 0.8, and 0.999 showing peaks primarily due to $m=l$ angular modes at frequencies $\omega \simeq m\omega_H$.

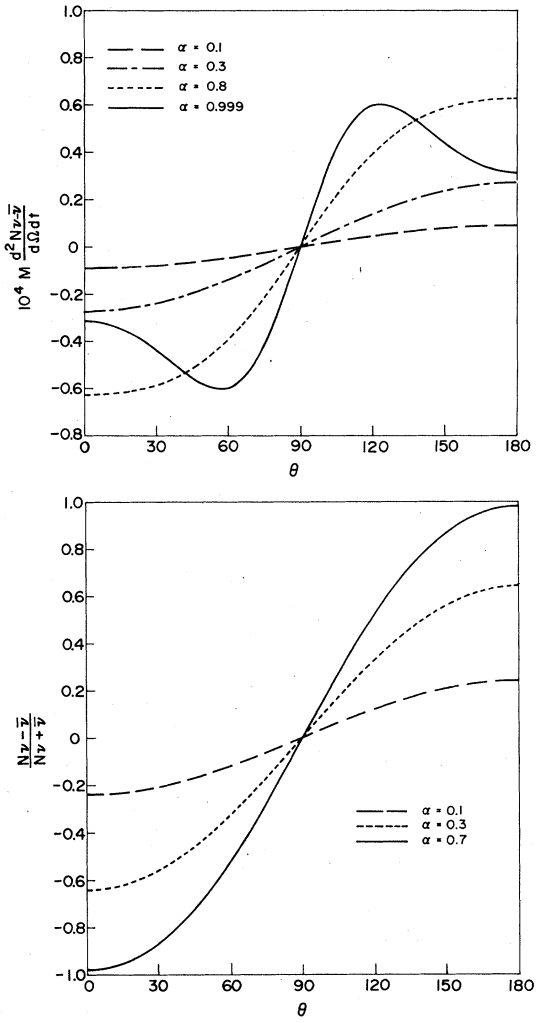

FIG. 3. (a) Net number rate (neutrinos minus antineutrinos) vs polar angle θ for $\alpha = 0.1$, 0.3, 0.8, and 0.999. (b) Asymmetry vs θ for $\alpha = 0.1$, 0.3, and 0.7. Asymmetry is the difference divided by the sum of neutrino and antineutrino rates.

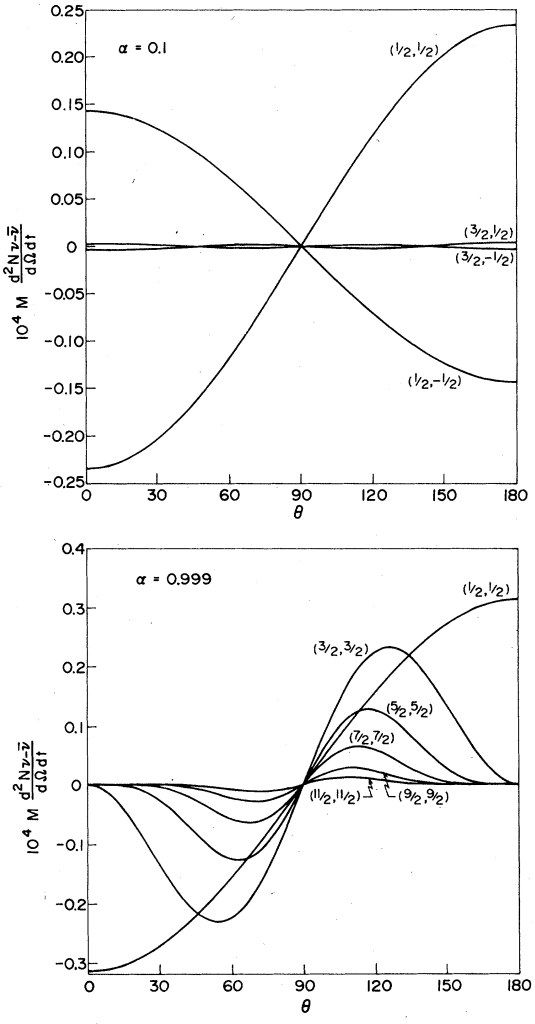

FIG. 4. (a) Net number rate vs θ plotted separately for the dominant (l, m) angular modes for $\alpha = 0.1$. (b) Same as (a) but for $\alpha = 0.999$.

closely approximating a $\cos\theta$ dependence. The asymmetry always peaks at the poles.

The net neutrino number emission rate, on the other hand, does not peak at the poles for $\alpha \gtrsim 0.8$. The peak in the current away from the poles for $\alpha \gtrsim 0.8$ is due to the increasing dominance of the higher l modes in the emission seen in Fig. 2. For $\alpha \lesssim 0.8$ the net rate increases monotonically with α for all angles θ, with the peak at the poles indicating the dominance of the $l = \frac{1}{2}$ mode.

To give a more detailed picture of the contributions to the angular dependence of the net neutrino current of the various l modes, these have been plotted in Fig. 4 for $\alpha = 0.1$ and 0.999. For $\alpha = 0.1$ we see that only the $l = \frac{1}{2}$ mode is significant, but both $m = \frac{1}{2}$ and $m = -\frac{1}{2}$ modes contribute. Their contribution to the net rate almost cancels, giving a small net flux of neutrinos. Since the contribution to the total number current is the absolute value of the net rate for each of the modes, one sees also that for small α the fractional asymmetry will be small.

For $\alpha = 0.999$, however, the higher l modes also contribute, with $m = l$ being the only significant modes. Here very little cancellation between different modes occurs except near the equator, giving large fractional asymmetry.

The power emitted by the black hole (2.13c) is plotted in Fig. 5. The increase with α is steady. For $\alpha \gtrsim 0.8$ the emission at the poles drops. The emission rate for neutrinos plus antineutrinos $Md^2N_{\nu+\bar{\nu}}/d\Omega dt$ has not been plotted, but behaves similarly to the power in Fig. 6. Because of the

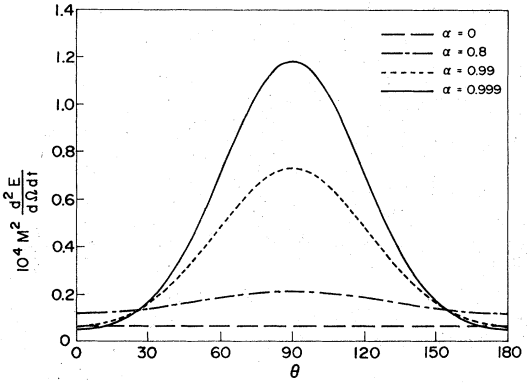

FIG. 5. Power in neutrinos plus antineutrinos vs θ for $\alpha = 0$, 0.8, 0.99, and 0.999.

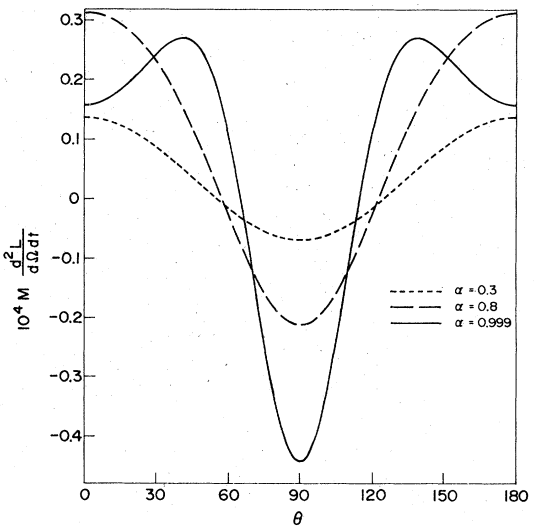

FIG. 6. Angular momentum loss rate vs θ in the form of emitted neutrinos and antineutrinos for $\alpha = 0.3$, 0.8, and 0.999.

hardening of the spectrum near the equator, it does not rise, with increasing α, as fast as the power does for $\theta \sim \pi/2$. The mean energy per neutrino $\bar{\omega}$ varies from $M\bar{\omega} \simeq 0.18$ for $\alpha = 0$ to $M\bar{\omega} \simeq 0.8$ for $\alpha = 0.999$, though because of the sharp peaks in the spectrum (Fig. 2) and the dependence of the spectrum on θ, $\bar{\omega}$ has little relevance for large α.

The angular momentum loss rate (Fig. 6) displays general behavior similar to Figs. 3(a) and 5. It is negative at the equator but the total loss rate integrated over angle is positive and increases with α.

This process of asymmetric neutrino emission from Kerr black holes provides a means of converting an initial amount of angular momentum into a separation of lepton number (see also Ref. 6). This could provide a mechanism for producing matter-antimatter separation in an initially baryon symmetric universe to explain the observed (local) nonzero baryon number. This has been investigated and the results will be reported elsewhere. However, the conclusion there seems to be that this effect is many orders of magnitude too small to account for our present universe.

ACKNOWLEDGMENTS

We would like to thank the N.S.E.R.C. of Canada for partial support under Grant No. 67-0441. One of us (W.G.U.) would also like to thank the Alfred P. Sloan Foundation for its support. We would also like to thank D. Page for giving us some of his unpublished results. D.A.L. was the recipient of an N.R.C. 1967 Science Scholarship.

[1]S. Hawking, Nature 248, 30 (1974); Commun. Math. Phys. 43, 199 (1975).
[2]D. Page, Phys. Rev. D 13, 198 (1976).
[3]Helicity is the scalar product of a particle intrinsic spin ($\vec{\sigma}$) with its momentum ($\vec{p}$):
$$\frac{\vec{\sigma}\cdot\vec{p}}{(p^2+m^2)^{1/2}}\,.$$
[4]Experimentally it is known only that weak interactions violate parity maximally. Positive-helicity neutrinos could exist and thus be produced in black-hole evaporation. As they would not interact with matter except gravitationally, we will omit them from further consideration.
[5]W. Unruh, Phys. Rev. Lett. 31, 1265 (1973).
[6]A. Vilenkin, Phys. Rev. Lett. 41, 1575 (1978); 42, 195(E) (1979).
[7]D. Page, Phys. Rev. D 14, 3260 (1976), has calculated rates integrated over angle in his discussion of evolution of rotating black holes.
[8]C. Misner, K. Thorne, and J. Wheeler, *Gravitation* (Freeman, New York, 1970).
[9]D. Brill and J. Wheeler, Rev. Mod. Phys. 29, 465 (1957).
[10]S. Detweiler and J. Ipser, Astrophys. J. 185, 675 (1973).
[11]W. Unruh, Phys. Rev. D 10, 3194 (1974).
[12]S. Fulling, J. Phys. A 10, 917 (1977).
[13]W. Unruh, Phys. Rev. D 14, 870 (1976).
[14]B. Carter, Phys. Rev. 141, 1242 (1966); 174, 1559 (1968).
[15]E.g., S. Schweber, *An Introduction to Relativistic Quantum Field Theory* (Harper and Row, New York, 1961).
[16]W. Press and S. Teukolsky, Astrophs. J. 185, 649 (1973).
[17]E.g., M. Abramowitz and I. A. Stegun, *Handbook of Mathematical Functions* (Dover, New York, 1965).
[18]D. Page, private communication.
[19]D. Page, Phys. Rev. D 16, 2402 (1977).
[20]University of British Columbia Computing Centre, Documentation: U. B. C. DE (Subject Code 43.2) (unpublished).